

## An *In Silico* Approach to Define Potential Biomarkers of miRNA-Associated ceRNAs for Breast Cancer

Serap Ozer Yaman <sup>1,a,\*</sup>, Sema Mısır <sup>2,b</sup>

<sup>1</sup> Department of Medical Biochemistry, Faculty of Medicine, Karadeniz Technical University, Trabzon, Türkiye.

<sup>2</sup> Department of Biochemistry, Faculty of Pharmacy, Sivas Cumhuriyet University, Sivas, Türkiye.

\*Corresponding author

### Research Article

#### History

Received: 06/01/2023

Accepted: 17/03/2023

#### Copyright



©2023 Faculty of Science,  
Sivas Cumhuriyet University

### ABSTRACT

Breast cancer (BC) is the most common type of cancer with the highest incidence in women. Particularly in breast cancer, competing endogenous RNAs (ceRNAs) play crucial roles in a variety of metabolic pathways including proliferation, migration, and apoptosis. The aim of the present study is to identify combinatorial target genes (ceRNAs) by employing *in silico* research to identify miRNAs specific to BC. The other aim was to determine possible biomarkers for the diagnosis of BC by selecting those containing the Transcribed Ultra Conserved Region (T-UCR). Using the miRWalk database, 40 miRNAs that have been experimentally shown to be clinically linked with BC were found. T-UCR-containing genes with potential ceRNA activity were identified. Genes with statistically significant changes in expression between BC and normal breast tissue were identified using the GEPIA. The relationship of the *CLK3* and *NFAT5* genes was found using the Spearman correlation test. The Spearman correlation test was used to determine the association between the *CLK3* and *NFAT5* genes, and the genes were found to be significantly less expressed in BC. The *NFAT5* and *CLK3* gene pair have been found to be associated with BC ( $p < 0.001$ ;  $r = 0.35$ ), and may function as useful biomarkers for BC.

**Keywords:** Biomarker, Breast cancer, ceRNA, miRNA.

 [serapozer@ktu.edu.tr](mailto:serapozer@ktu.edu.tr)

 <https://orcid.org/0000-0002-5089-0836>

 [smisir@cumhuriyet.edu.tr](mailto:smisir@cumhuriyet.edu.tr)

 <https://orcid.org/0000-0002-5919-3295>

## Introduction

Breast cancer (BC) accounts for 25.2% of all female cancers in the world. The prevalence of female cancer is highest in BC, and rates are rising quickly [1]. BC is a complex disease that greatly strains human health and reduces the quality of life. In 2018, it is predicted that there were 626.679 BC related deaths (6.6% of 9.6 million deaths) and 2,088,849 newly recognized BC cases (11.6% of 18.1 million new cases) [2]. Among the imaging medical diagnostic methods used for the early detection of BC, the only clinically proven test method is mammography [3]. The prevalence and fatality of BC highlight the importance of studying the processes behind the breast cancer development as well as developing new methods of diagnosis and therapy [3, 4].

A group of non-coding RNAs with a length of 18–22 nucleotides are called microRNAs (miRNAs) which acts as post-transcriptional modulators of gene expression. miRNAs bind directly to the mRNA of the target molecule, regulating gene expression by inhibiting translation and causing mRNA degradation. Finding important miRNA targets for cancer research is crucial because each miRNA has the ability to regulate hundreds of target genes. [5]. By targeting the expression of oncogenes or tumor suppressor genes, miRNAs have been shown to play vital roles in the genesis, development and progression of BC. To determine the roles of miRNAs in BC, it is necessary to examine miRNA expression profiles between normal and tumor tissues, then to understand differentially expressed miRNAs [6].

By competing with one another for miRNAs, transcripts known as competing endogenous RNA (ceRNAs) can regulate one another at the post-transcriptional level. CeRNA connections link the roles of non-coding RNAs such as microRNA, long non-coding RNA, pseudogenetic RNA, and circular RNA to those of protein-coding mRNAs. CeRNAs, which are transcripts that have the miRNA response element, can be used to regulate post-transcriptional gene expression in both health and disease. Numerous elements, including the quantity and subcellular location of ceRNA components, the affinity of miRNAs to their sponges, RNA sequences, and regulation, all have an impact on ceRNA function. Differences in these factors can release ceRNA networks and thus cause many pathological conditions, including cancer [7].

In recent years, non-coding RNAs (ncRNAs) have attracted major interest in cell transformation. By comparing the genomes of the mouse, rat, and human using bioinformatics tools, ultra-conserved regions (UCRs) were identified in 2004. UCRs consist of at least 481 genomic sequences between 200–779 bp lengths that are strictly conserved across the three vertebrate species. Although the function of T-UCRs is not fully known, it is stated that their conservation across the species is important for mammalian ontogenesis/phylogenesis. T-UCRs have diverse profiles in different types of human malignancies, according to the current genome profiling research, which further supports their significance in human carcinogenesis [8].

MiRNAs, which are well-known to play a crucial functional role in cancer, have promised hope in elucidating the molecular pathophysiology of the disease and creating molecularly targeted treatments.

The aim of this study is to determine BC-specific miRNAs, find combinatorial target genes (ceRNAs), select among them those containing the Transcriptionally Ultra Conserved Region (T-UCR) among them, and identify potential predictive biomarkers for BC diagnosis by *in silico* analysis.

## Methods

### Identification of miRNAs in BC

Forty miRNAs that have been experimentally proven to be clinically associated with BC were identified using the miRWalk database. The anticipated and verified information on miRNA-target interaction is available from the miRWalk database. The "Validated Target module" utilized in this study is updated every month [9].

### Identification of BC-specific miRNA-mediated ceRNAs

1009 genes predicted to be characterized by these 40 miRNAs simultaneously were found using ComiR (combinatorial microRNA database), and 869 genes with a ComiR score above 0.911 were taken into consideration. The combinatorial arrangement of miRNA pairs of the observed transcriptome was determined. In line with the results obtained, comprehensive ones for combinatorial editing by miRNAs are presented. The probability of combinatorial miRNA activity was estimated in annotating data with the ComiR score. Therefore, combinatorial arrangement and statistical constraints were applied to recover the correct miRNA in BC and identify hundreds of genes from miRNA sets. ComiR is a web tool for predicting the targets of miRNAs. ComiR calculates the potential for targeting by a set of miRNAs, each of which may have one or more targets in its 3' untranslated region. ComiR utilizes user-provided miRNA expression levels [10].

### Determination of BC-associated ceRNA with genes including T-UCR

T-UCRs play role in the development of many diseases, including cancer. For this reason, it was ensured that these genes were matched. Therefore, the data of the study by Bejerano et al. were taken as a basis, and genes containing T-UCR in their exonic regions were determined [11].

### Differential Expression of Genes in Breast Cancer and Healthy Tissues

Based on data from the Genotype-Tissue Expression (GTEx) and Cancer Genome Atlas (TCGA), GEPIA is an interactive web application. Many visualization and analysis tools for gene expression have been made available by GEPIA. Using the gene expression profiling database GEPIA, we discovered *NFAT5* and *CLK3* genes among breast cancer-associated ceRNAs, including T-UCR, with significant expression changes between BC and normal breast tissue.

Distribution of *NFAT5* and *CLK3* gene expressions according to TCGA normal and GTEx data in GEPIA was performed using ANOVA. And also,  $|\text{Log2FC}|$  Cutoff:1 and q-value Cutoff: 0.01 were taken [12].

### Correlation analysis of *NFAT5* and *CLK3* genes

Using the Spearman correlation test in the GEPIA, a comparison of the *NFAT5* and *CLK3* genes in BC and normal breast tissue was performed [12].

Figure 1 shows the schematic flow chart illustrates the general methodology including miRNA selection, miRNA-mediated ceRNAs analysis, matching of ceRNAs with the genes containing T-UCR and correlation analysis.

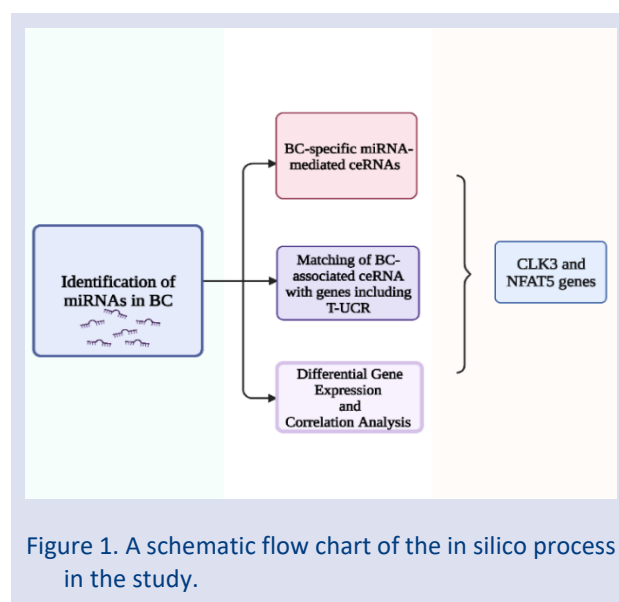


Figure 1. A schematic flow chart of the in silico process in the study.

## Results

40 miRNAs that have been experimentally proven to be associated with breast cancer (MCF-7) were detected. 1009 genes targeted simultaneously by these 40 miRNAs were identified and 869 genes with a ComiR score above 0.911 were considered (Table 1, 2, 3).

Table 1. List of miRNAs involved in MCF-7 cells

hsa-let-7f-5p	hsa-miR-10b-5p	hsa-miR-1226-3p	hsa-miR-7-5p	hsa-miR-145-5p	hsa-miR-21-5p
hsa-miR-146b-5p	hsa-miR-155-5p	hsa-miR-196a-5p	hsa-miR-520e	hsa-miR-185-5p	hsa-miR-17-5p
hsa-miR-196b-5p	hsa-miR-199b-5p	hsa-miR-200a-3p	hsa-miR-22-3p	hsa-miR-205-5p	hsa-miR-206
hsa-miR-20a-5p	hsa-miR-146a-5p	hsa-miR-200b-3p	hsa-miR-221-3p	hsa-miR-222-3p	hsa-miR-27a-3p
hsa-miR-27b-3p	hsa-miR-299-5p	hsa-miR-29a-3p	hsa-miR-29b-3p	hsa-miR-328-3p	hsa-miR-328-5p
hsa-miR-339-5p	hsa-miR-342-3p	hsa-miR-345-5p	hsa-miR-375	hsa-miR-451a	hsa-miR-520b
hsa-miR-181b-5p	hsa-miR-125b-5p	hsa-miR-9-3p	hsa-miR-92a-3p		

Table 2. Genes likely to show the highest ceRNAs function for 40 miRNAs by the ComiR.

Gene ID	Comir equal abundance score	Gene ID	Comir equal abundance score	Gene ID	Comir equal abundance score	Gene ID	Comir equal abundance score
CFLAR	0.9233	GAS7	0.9182	AGPS	0.9111	SLC39A9	0.9115
SLC7A2	0.9148	CDKL5	0.9228	PRDM11	0.9144	IKZF2	0.9191
SARM1	0.9197	REV3L	0.9224	MRE11A	0.913	PIAS1	0.9143
LIG3	0.9123	IYD	0.9206	NDUFS1	0.9192	DAPK2	0.9144
KMT2E	0.9149	ZNF207	0.9226	KPNA6	0.9185	CYP46A1	0.9113
MAP3K9	0.9168	BRCA1	0.9168	AGPAT4	0.9197	INPP4A	0.9206
FARP2	0.9119	NUDCD3	0.9191	POU2F2	0.9135	ADAM28	0.911
DCUN1D1	0.9135	HDAC9	0.9176	RSF1	0.9187	CELF2	0.9173
ADAMTS6	0.9189	H6PD	0.9191	KIAA2022	0.9135	SLC4A8	0.9206
HEBP2	0.9203	ALX4	0.9156	AP5M1	0.9207	FAM168A	0.918
EIF2AK2	0.9168	KMT2C	0.9239	PRDM6	0.9152	NCKAP1	0.9233
MON2	0.9198	EPN1	0.9236	CDON	0.9123	HIPK2	0.9227
GNAI3	0.9241	WDR3	0.9126	TRAM2	0.9195	SNAP91	0.9138
CYB5R4	0.9183	GSTO2	0.9159	SLC9A7	0.9172	CD84	0.9178
ATXN3	0.9241	MYO9A	0.9119	RRP15	0.9166	POLR1A	0.9137
RORA	0.9216	GNB5	0.9222	SLC44A1	0.9116	EXOC5	0.9161
MGAT4A	0.917	MBD3	0.9154	ZFYVE26	0.9134	SMC1A	0.9151
CHFR	0.9224	TRHDE	0.9201	AP1M1	0.9216	MAP3K13	0.916
RASAL2	0.9233	ZNF37A	0.9114	FNDC3B	0.9137	BCAP29	0.911
RBM7	0.9112	RBMS2	0.9145	PAG1	0.9179	MBNL3	0.9222
PPP1R12B	0.9233	DNAJC10	0.9238	DCX	0.9188	ACER3	0.9171
PIK3C3	0.9143	N4BP2	0.9202	SAR1A	0.9163	STX7	0.9222
RFX3	0.9113	RAB21	0.9234	CDH7	0.9153	PGR	0.9205
FAM135A	0.911	TRPM3	0.9205	TNPO1	0.9167	DIS3	0.9187
ZNF264	0.9214	REST	0.9115	SSH1	0.9205	ATRX	0.9154
HSD17B2	0.9213	SH3BP2	0.9197	C14orf166	0.9204	MAVS	0.9226
ZBTB25	0.9229	GPATCH2L	0.9231	ZNF268	0.923	PDPR	0.9151
TNRC6A	0.9228	WDR7	0.9192	RGS17	0.9189	AGO1	0.9214
RFFL	0.9122	SEC22C	0.9195	CBX5	0.9211	FKBP5	0.9176
CECR2	0.9169	MAPK1	0.9207	ADRBK2	0.9152	MTMR3	0.9179
TNRC6B	0.9236	KIAA0930	0.9187	KCNK10	0.917	DDHD1	0.9227
SPTLC2	0.917	ZC3H14	0.9238	RPS6KA5	0.9241	RNF24	0.9167
RASSF2	0.9145	CDS2	0.9217	ST8SIA5	0.9234	CEP192	0.9197
LIPG	0.9188	XIAP	0.9143	PCYT1B	0.913	FGF14	0.9225
STK24	0.9219	DGKH	0.9237	INTS6	0.9235	NUP93	0.9134
NFAT5	0.9236	LONP2	0.9189	PLLP	0.9152	SLC7A6	0.9175
CMC2	0.9184	MLYCD	0.9211	USP31	0.9135	XYLT1	0.9126
HOMER2	0.9212	DTWD1	0.9223	BMF	0.9116	FZD3	0.923
UBE2W	0.9152	NOVA2	0.9136	AVL9	0.9148	GTPBP10	0.917
CDK6	0.9218	ITGB8	0.9195	FKBP14	0.9123	PLEKHA8	0.9199
ZKSCAN1	0.9187	RBM28	0.9237	TMEM106B	0.922	PSMA2	0.9144
FKTN	0.9178	FSD1L	0.9165	MEGF9	0.9143	TRDMT1	0.9229
PLEKHA1	0.9231	CCSER2	0.912	BMPR1A	0.9192	CPEB3	0.9184
SH3PXD2A	0.9188	TSPAN14	0.9239	NUFIP2	0.9202	FBXL20	0.9184
TMEM33	0.9134	GABRA4	0.9162	USP46	0.92	GAB1	0.914
TRIM2	0.916	WHSC1	0.9144	CBL	0.9218	KIAA1549L	0.9134
SLC1A2	0.9205	SOX6	0.9177	CAPRIN2	0.9213	PPM1H	0.9147
KCNA1	0.9199	C12orf49	0.9195	CAND1	0.9126	KRR1	0.9207
FRK	0.9232	SOD2	0.9236	MDEGA1	0.9137	ZNF451	0.9161
BAG2	0.9112	KIAA1244	0.9209	SLC16A10	0.9227	PHACTR2	0.9145
QKI	0.9188	SEMA5A	0.9198	RNF130	0.9162	CNOT6	0.9145
LNPEP	0.9179	PRLR	0.9184	SKP1	0.9192	HEMK1	0.9237
ACVR2B	0.9228	NKTR	0.9137	FOXP1	0.912	INO80D	0.9216
TTL	0.923	TFCP2L1	0.9137	GGCX	0.915	KDM3A	0.916
ZNF142	0.9147	STRN	0.9124	KYNU	0.9235	AAK1	0.924
PLEKHA3	0.9234	TNR	0.9137	QSOX1	0.9125	KCNC4	0.9238
C1orf21	0.921	SLC35D1	0.912	TTF2	0.9159	LGALS8	0.9121
MTR	0.9166	RIMS3	0.9186	DR1	0.9202	PTBP2	0.9214
DIEXF	0.9114	ATF6	0.9184	CREB1	0.915	KLF7	0.9198
PHF3	0.9114	FBXO30	0.9113	MED28	0.9228	SLC16A7	0.9228
KLF12	0.9203	CCND2	0.9158	CYP20A1	0.9209	FBXW2	0.9145
ONECUT2	0.9238	DNAL1	0.9201	NRDE2	0.9221	DNMT3A	0.9145

YIPF4	0.9227	OGFRL1	0.9151	PANK3	0.9202	PLXDC2	0.9218
DNAJC15	0.9167	KDM3B	0.9123	PAPD5	0.9166	ZMYM2	0.9123
PIK3CA	0.9122	GTDC1	0.9221	SV2C	0.9196	RPAP2	0.9236
FAM126A	0.9196	KIAA1549	0.9135	SLC25A16	0.9119	RASSF8	0.9141
NCKAP1L	0.9124	ACVR1C	0.916	LPGAT1	0.9182	VAPB	0.9115
RAB22A	0.9217	NQO2	0.9184	SSR1	0.9192	ATXN1	0.9217
ATP5S	0.9188	GTF3C4	0.9143	PSD4	0.9179	OPA3	0.919
AP5S1	0.9146	CEP250	0.9222	AGO3	0.9236	KLC1	0.9233
PCNXL4	0.9218	PLEKHG3	0.9178	HELB	0.9219	RAP1B	0.9234
RAB3IP	0.9195	PTPRB	0.9112	DYRK2	0.9171	SLC35E1	0.9126
HIP1	0.9132	ZNF780B	0.9159	PODXL	0.9163	FOXP2	0.9209
MKLN1	0.9212	PDE11A	0.9165	TMOD2	0.9219	TTBK2	0.9172
C15orf57	0.9142	ICE2	0.9114	FAM63B	0.9152	MAS1	0.9217
PGPEP1	0.9172	RAB11FIP4	0.9181	RLIM	0.9159	CHRM3	0.9166
SCO1	0.9179	MPRIP	0.9202	FAM83F	0.9235	TMTC1	0.9149
MBD2	0.9142	SORT1	0.9172	WNT2B	0.9216	KIDINS220	0.9165
NAV1	0.9136	EMP1	0.9133	KLRD1	0.9231	DSC2	0.921
C5AR2	0.9122	CLOCK	0.9202	APC	0.9185	MTO1	0.9192
PRRG4	0.9118	GDF11	0.9145	ESPL1	0.9182	USP15	0.9234
GNS	0.9114	MDM2	0.9223	NTPCR	0.9142	KIAA1614	0.9135
RC3H1	0.9152	TMEM127	0.9113	GCC2	0.9177	ALDH1L2	0.9166
ITM2B	0.9147	TNS3	0.9156	DBNL	0.9188	ALPK3	0.9142
DCAF7	0.9157	KAT7	0.9168	UGGT1	0.9152	GOLGA1	0.9114
TAF8	0.9165	RAB30	0.9199	SLCO5A1	0.917	UNC13C	0.9151
PAQR5	0.9116	DBT	0.9205	EPT1	0.9177	ENTPD1	0.9213
SSFA2	0.9142	ABI2	0.9241	USP8	0.9239	TMOD3	0.9194
KIAA1644	0.9196	FGD4	0.9112	NDUFA9	0.9211	LLPH	0.9166
TMEM132B	0.9168	SLC7A1	0.9121	ANKRD52	0.919	ZNF740	0.9137
WDFY2	0.9213	NOVA1	0.9205	SYT16	0.9227	NAA30	0.9151
KCNH5	0.9201	SLC24A4	0.9192	TSPAN3	0.9158	IGF1R	0.9152
ABHD2	0.9205	NTRK3	0.9235	FTO	0.9211	VPS53	0.9233
RNF165	0.9161	NFIC	0.9206	FEM1A	0.9181	WTIP	0.9229
CACNG8	0.9115	GPR161	0.9123	POU2F1	0.9231	ILDR2	0.9206
SDHC	0.9234	ABL2	0.9232	TOR1AIP1	0.9144	SNX27	0.9145
GABPB2	0.9196	SYT14	0.9199	KCNN3	0.9223	GATAD2B	0.9134
LYST	0.9192	MBOAT2	0.915	SYT2	0.9145	ASXL2	0.9173
KIAA1715	0.9159	LIMD1	0.9196	LPP	0.9237	STXBP5L	0.9112
ANK2	0.9159	SPATA5	0.9162	SETD7	0.9142	MARCH6	0.9172
RPL37	0.922	SSBP2	0.9178	PPI5K2	0.9203	ARHGAP26	0.916
G3BP1	0.9138	GFOD1	0.9136	FAXC	0.9199	CLVS2	0.918
RNF217	0.9212	SHPRH	0.9207	CREB5	0.9145	EGFR	0.9208
PURB	0.9161	TMEM168	0.9119	LANCL3	0.9216	CASK	0.9123
FBXO25	0.9154	WHSC1L1	0.9159	MTDH	0.9127	VLDLR	0.9176
NFIB	0.9151	CEP78	0.9192	NTRK2	0.9144	SNX30	0.9203
NR6A1	0.9188	USP6NL	0.9179	ZEB1	0.9205	EIF4EBP2	0.916
NPFFR1	0.9215	LRRC27	0.9164	CNNM2	0.923	CELF1	0.9177
SESN3	0.9137	SOGA1	0.9162	HMGA2	0.9173	CDH8	0.9172
LPHN3	0.9182	CD226	0.9197	FREM2	0.9135	SLC7A11	0.9187
THRB	0.9134	DLG5	0.911	GXYLT1	0.9188	EIF4E	0.9199
AKAP6	0.9198	MIPOL1	0.9166	FER	0.9214	WWC2	0.9181
GABRA2	0.9133	GFRA1	0.9153	CACUL1	0.9199	PTPN14	0.9199
MGAT5	0.9151	PDK1	0.9227	UHMK1	0.9182	GUCY1A2	0.9227
JMY	0.9124	CCDC50	0.9135	CAMK4	0.9199	GPR180	0.9182
FARP1	0.9152	RAB3C	0.921	SREK1IP1	0.9134	MR1	0.9136
BCL2L11	0.9119	ASAP1	0.9112	PLEKHG4B	0.9216	CNKSR3	0.924
DGKE	0.9134	HS2ST1	0.9157	CHST9	0.9213	ANKH	0.9113
OTULIN	0.9195	LRRK1	0.9226	ENAH	0.9213	PDE1C	0.9177
ADAMTS5	0.9113	TTC39B	0.9183	GOLGA7B	0.9112	MIER3	0.911
FAM126B	0.9167	PPARGC1B	0.9187	SLC24A2	0.922	AFF2	0.9222
PSD3	0.9127	MMP16	0.9215	KCNMA1	0.9127	PPP2R2B	0.9212
SAMD8	0.918	RAB11FIP1	0.9165	UNC5D	0.9113	MPV17L	0.911
ST3GAL2	0.9112	KCNJ6	0.9238	ZNF618	0.9201	DGKI	0.9162
UBN2	0.9213	BRAF	0.9161	AGAP1	0.9224	CLSTN2	0.9221
KCNB1	0.9214	ELK4	0.9197	ADAMTS4	0.9197	IGF2BP1	0.9181
ZBTB8A	0.914	KALRN	0.9186	PDXK	0.9124	ICOSLG	0.9182
TAOK1	0.9214	ORAI2	0.9207	IKZF3	0.9207	EMC10	0.9138

FMNL3	0.9219	PRKAA2	0.9195	GMEB1	0.9137	DRAXIN	0.9142
RBBP4	0.9124	NFIA	0.9206	ZNF326	0.9178	SLC30A7	0.9159
DDR2	0.9136	ACP6	0.9124	KIF26B	0.9171	REL	0.9207
DISC1	0.9124	PAQR3	0.9205	EIF4E3	0.9222	LRRCS58	0.9124
PPM1L	0.9219	ICA1L	0.9113	RYBP	0.9166	GMPS	0.9207
SMIM14	0.9133	RPP14	0.9136	APBB2	0.9143	ZNF148	0.9124
GRIK3	0.9113	LRPAP1	0.9169	UBXN7	0.9184	INTU	0.9224
HSPA4L	0.9201	RAD54L2	0.9112	RICTOR	0.9125	CCDC127	0.9184
CREBRF	0.9156	SAP30L	0.911	KIF6	0.9197	USP49	0.916
ZNF704	0.9239	ADCY1	0.9216	FOXK1	0.9138	KIAA1958	0.9192
PTCHD1	0.9229	BRWD3	0.9149	SLITRK5	0.9238	CFL2	0.918
SUGT1	0.9238	PGM2L1	0.9165	AMER2	0.9195	PDZD8	0.9176
FAM204A	0.922	NSD1	0.9147	TSC1	0.9191	FUNDC2	0.9159
TTC7B	0.9236	CPSF2	0.9207	CLMN	0.9189	HIF1AN	0.9237
FRS2	0.9148	ARIH1	0.924	STXBP4	0.9217	TRIM44	0.9227
TUB	0.9147	PLD4	0.9142	TRIM66	0.9213	RNF169	0.9134
PRTG	0.9224	PRKCB	0.9185	TMED3	0.9232	GALR1	0.9216
SLFN5	0.9187	DCTN5	0.9199	ELFN2	0.9113	GREM1	0.9232
FBXO22	0.9188	TBC1D16	0.9205	IRGQ	0.9137	ZNF226	0.9159
ANKRD11	0.9187	ZNF641	0.9144	TTYH1	0.9155	SLC43A2	0.9181
HOOK3	0.9226	MPLKIP	0.9114	LDLRAD4	0.9194	SNTB2	0.9207
SPRY3	0.9137	IRS1	0.9122	MECP2	0.9225	AR	0.9211
CSNK1G1	0.9172	RAB3B	0.9232	SH3TC2	0.9171	SHE	0.9171
C15orf40	0.9219	HIC2	0.9154	OTUD7A	0.9192	KLF13	0.9121
MAP3K2	0.9218	TMEM154	0.9179	TMEM192	0.9214	ZNF778	0.9162
NIPA1	0.9148	SIK2	0.9124	RNF150	0.9183	CRTAP	0.917
LONRF2	0.9229	ELOVL6	0.9179	NUDCD2	0.9172	SGCD	0.9137
ATF7	0.9134	TANC2	0.9135	PYGO1	0.9166	KCNMB3	0.9169
CLCN5	0.9198	KSR2	0.9234	ZNF562	0.9226	WIPF2	0.9134
BCL2	0.9141	NEGR1	0.9218	ALG14	0.9198	FUT9	0.9226
ZNF24	0.9145	ZMAT3	0.9145	DCP2	0.9198	BNC2	0.9221
VANGL1	0.9188	GOLGB1	0.9232	STOX2	0.9114	PEAK1	0.9239
GMPPB	0.911	SNX33	0.9123	NABP1	0.9212	NUDT4	0.9153
SCAI	0.9162	HEG1	0.9168	AGFG1	0.9166	RNF213	0.9134
ZNF791	0.9204	PHC3	0.923	UBXN2A	0.9137	ZHX3	0.9152
CNTNAP2	0.918	C4orf32	0.9188	FZD4	0.9124	PDE12	0.9187
CA5A	0.9216	CADM2	0.9183	SMAD2	0.9241	ARL10	0.9214
PPP2R2D	0.9229	MLXIP	0.9149	SLC35E3	0.9237	ZDHHC21	0.9192
KCMF1	0.9113	SPRYD4	0.9203	SYNE3	0.9234	KIAA2018	0.9126
SOX11	0.9161	POLE	0.9135	ZBTB34	0.9162	RIMKLA	0.9202
NR2C2	0.9212	ST8SIA3	0.921	SAMD12	0.9195	PGBD5	0.923
ZBTB41	0.9139	FAM26E	0.9162	PDE4DIP	0.9141	GEN1	0.9126
NT5DC1	0.9168	CD28	0.9113	ERBB4	0.9211	ERN1	0.9149
CSRNP3	0.9162	CLK3	0.9221	CIITA	0.9198	SERTAD2	0.9129
SOCS4	0.9111	ZADH2	0.9186	ZNF609	0.9111	SSTR2	0.9122
YOD1	0.9207	LRRCS57	0.9202	EHMT1	0.9181	PLAG1	0.9122
RFX7	0.915	IBA57	0.9209	MGAT4C	0.9237	CREB3L2	0.9201
UNC5C	0.9125	RGMA	0.9218	EXT1	0.9168	BACE2	0.9114
GABRG3	0.9174	FIGN	0.9219	CLN8	0.9179	PAPPA	0.9133
NGRN	0.9142	C16orf72	0.9228	GJC1	0.9192	CADM1	0.9211
SLC8A1	0.9239	CALN1	0.9173	POTEC	0.919	CTNNA3	0.9115
GRIN2A	0.9225	MACC1	0.9124	KCTD16	0.9229	B3GALT5	0.9229
BTBD9	0.9177	KCNH8	0.9137	KCNQ3	0.9173	PCDH9	0.924
ZBTB40	0.9132	SDR42E1	0.9226	ZFP90	0.9136	FAM227A	0.922
BRI3BP	0.9133	FLRT2	0.9241	PURA	0.9229	ZBTB37	0.924
HS6ST3	0.9144	RAD51D	0.9192	GPRIN3	0.9207	SV2B	0.9146
LSAMP	0.9168	OLFML2A	0.912	PBX1	0.9112	C16orf52	0.9149
PIGP	0.9187	PTCH1	0.9216	LRCH3	0.9156	MKL2	0.9175
ZNF555	0.9192	KPNA4	0.9172	PPARA	0.922	TEAD1	0.9168
NAP1L1	0.923	SESTD1	0.9153	TET3	0.9135	ZNF286A	0.912
LIN28B	0.914	NWD1	0.9172	ZNF383	0.9145	CENPP	0.9204
ASAH2	0.9121	PTAR1	0.9205	VWC2	0.9169	TMEM120B	0.9203
MTF1	0.917	BEND4	0.9145	LRRK2	0.9134	PTPLAD2	0.9145
ZNF527	0.9155	FAM179A	0.9221	PTPRT	0.9198	LCOR	0.9214
XPNPEP3	0.9193	ZNF765	0.9172	TSC22D2	0.9115	ZNF605	0.9226
MYO18A	0.9181	AJAP1	0.9196	HDAC2	0.9126	WNK3	0.9176

ZNF431	0.922	VKORC1L1	0.9168	COL27A1	0.9134	NHLRC2	0.921
FLNA	0.9159	SRGAP1	0.924	ZNF470	0.9117	ZNF441	0.9119
GMFB	0.921	PGAP1	0.9161	ZNF720	0.9158	DDI2	0.9214
LRP10	0.9153	ZNF655	0.9157	SPN	0.9149	MYO5A	0.9151
FAM212B	0.9122	ZNF121	0.9142	MPZL1	0.9143	MBP	0.9226
DLGAP2	0.9221	MRPL42	0.9237	ZNF544	0.9116	CACNA1E	0.9212
ZKSCAN8	0.9151	ASPH	0.9149	ZNF26	0.9233	NUDT16	0.9124
MDM4	0.9173	C6orf89	0.9165	IPO9	0.9221	SLC5A3	0.9222
FAM169A	0.9121	LRIG2	0.9162	RORB	0.9137	C1orf95	0.919
PHACTR4	0.9124	BMPR2	0.9192	MBD5	0.9179	FAM155A	0.9152
PCDHA4	0.9192	SLC35B4	0.9148	ZBTB10	0.9177	TMEM170B	0.9153
CCDC85C	0.9239	ITSN1	0.9226	ITPRIPL2	0.9133	DOK6	0.9182
TMEM200C	0.9173	CFAP44	0.9142	VGLL3	0.9153	TRIM71	0.9203
XKR4	0.9239	C17orf51	0.9223	SFT2D2	0.9221	FGFR1OP	0.9236
LEPROT	0.9119	DNASE1	0.9116	ZNF891	0.9225	LYRM4	0.9167
ZNF788	0.9134	PEX26	0.9235	SIAH3	0.9124	PLXNA4	0.9137
APOL6	0.9207	HSBP1	0.9183	TMEM189	0.9151	ARPIN	0.9178
FMN1	0.9207	ZNF286B	0.9119	PCDHA10	0.9224	KIAA1456	0.9177
SOGA3	0.9116	NOX5	0.9177	TIFAB	0.9123	CUX1	0.9221
<a>KIAA0408							
FRRS1L	0.9176	XKR7	0.9125	TMEM178B	0.9218	GAN	0.9235
DYNLL2	0.9177	OTUD7B	0.9124	RNF115	0.9198	TRABD2B	0.9192
GTF2H5	0.9167	NUDT3	0.9174	GRIN2B	0.9241	ZBTB8B	0.923
SOCS7	0.9124	NPHP3-ACAD11	0.9124	ZNF8	0.9204	CLN8	0.9179
ZNF229	0.9141						

Table 3: List of genes containing T-UCR in their exonic regions according to the study of Bejerano et al.

UCR number	Length (bp)	Gene (ID)
uc.143	218	AB014560
uc.203	203	AB067798
uc.135	201	AK096400
uc.339	252	ATP5G2
uc.413	272	BC060758
uc.49	207	BC060860
uc.61	326	BCL11A
uc.324	225	C11orf8
uc.285	232	CARP-1
uc.233	266	CENTG3
<b>uc.393</b>	<b>275</b>	<b>CLK3</b>
uc.185	411	CLK4
uc.184	230	CPEB4
uc.471	239	DDX3X
uc.331	218	DLG2
uc.13	237	EIF2C1
uc.194	201	EPHA7
uc.183	236	FBXW1B
uc.333	270	FLJ25530
uc.478	252	GRIA3
uc.479	302	GRIA3
uc.282	207	GRIN1
uc.97	442	HAT1
uc.144	205	HNRPDL
uc.186	305	HNRPH1
uc.263	207	HNRPK
uc.264	267	HNRPK
uc.443	239	HNRPM
uc.45	203	HNRPU
uc.46	217	HNRPU
uc.409	244	L32833
uc.174	260	MATR3

uc.129	212	MBNL1
uc.356	251	MBNL2
uc.375	300	MIPOL1
uc.292	217	MLR2
<b>uc.406</b>	<b>211</b>	<b>NFAT5</b>
uc.473	222	NLGN3
uc.378	251	NRXN3
uc.475	397	OGT
uc.280	220	PBX3
uc.338	223	PCBP2
uc.376	290	PRPF39
uc.377	217	PRPF39
uc.33	312	PTBP2
uc.102	338	PTD004
uc.48	298	PUM2
uc.477	209	RAB9B
uc.395	249	RBBP6
uc.330	207	RBM14
uc.455	245	RNPC2
uc.419	289	SFRS1
uc.138	419	SFRS10
uc.28	355	SFRS11
uc.189	573	SFRS3
uc.456	320	SFRS6
uc.50	222	SFRS7
uc.454	208	SLC23A1
uc.193	319	SYNCRIP
uc.436	210	TCF4
uc.414	246	THRA
uc.313	231	TIAL1
uc.208	218	TRA2A
uc.209	250	TRA2A
uc.77	296	ZFHX1B
uc.151	214	ZFR
uc.474	210	ZNF261

*NFAT5* (nuclear factor 5 of activated t cells), *CLK3* (dual specificity protein kinase 3) genes, which contain T-UCR and show ceRNA activity, were detected (Table 4).

Table 4. Breast cancer-associated ceRNAs, including T-UCR in their exonic region

Gene ID	BC	Normal breast tissue
<i>NFAT5</i>	4.29*	9.63
<i>CLK3</i>	36.03*	52.28

\*Significantly different between BC and normal breast tissues

This investigation revealed that the expression of the *NFAT5* and *CLK3* genes was considerably lower in breast cancer than in healthy breast tissue (Figure 2). GEPIA database was used for statistical analysis of the relationship between the *NFAT5* and *CLK3* genes and breast cancer (Figure 3).

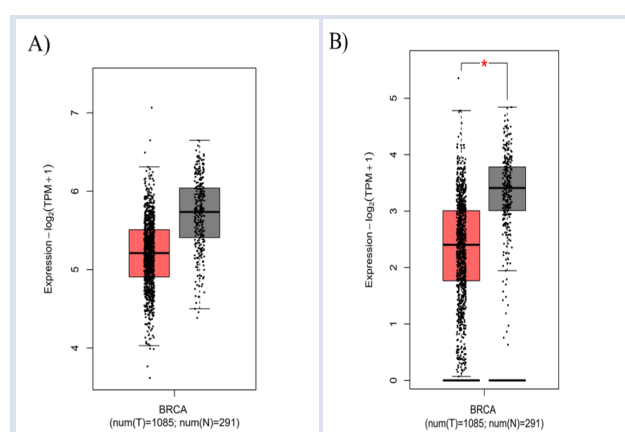


Figure 2. Distribution of *CLK3* and *NFAT5* gene expressions in BC and normal breast tissues according to TCGA normal and GTEx data in GEPIA. A) *CLK3*, B) *NFAT5* (BRCA: Breast cancer, T: tumour tissue, N: Normal breast tissue)

The *NFAT5* and *CLK3* gene pair has been found to be associated with breast cancer.

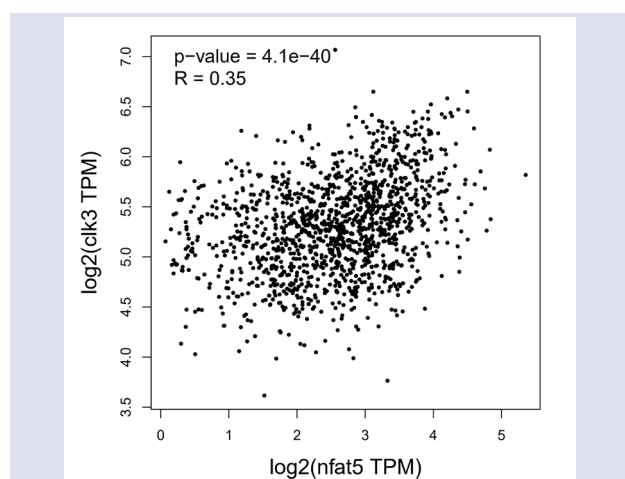


Figure 3. Spearman correlation analysis of *CLK3* and *NFAT5* genes in BC in the GEPIA

## Discussion

Breast cancer has a high incidence and mortality rate worldwide and is among the most common types of cancer [13]. To comprehend the mechanisms involved in the treatment, control, onset, and advancement of this disease, new prospective biomarkers must be discovered [14]. The determination of these molecules can contribute to the prevention and cure of the disease. Thus, an improvement in the quality of life of BC patients, and a decrease in mortality and morbidity can be observed [15, 16]. miRNAs have major functions in a variety of diseases, including cancers, where they act as oncogenes and/or tumor suppressors. Several studies have demonstrated that miRNAs regulate gene expression by interacting with multiple networks [17].

In recent years, a mechanism has been discovered that indicates that RNAs interact with each other [18]. The first time the ceRNA theory was put forth was by Salmena et al [19]. All RNA transcripts with miRNA binding sites are supposed to compete for post-transcriptional regulation, according to the competing endogenous RNA (ceRNA) hypothesis [19-22]. Endogenous competitive RNAs that regulate the binding of miRNAs to their targets have been identified [20], and this network established between miRNAs and ceRNAs has been expressed as ceRNA networks (ceRNET). As ceRNAs can act as regulators of miRNAs, ceRNAs may have an important role in miRNA-related diseases. Therefore, understanding the function of ceRNAs will provide understanding of the development process of diseases, including cancer, and the development of new treatment methods [18]. It has been stated that ceRNAs are important regulators in many cancer types [23]. Studies in the literature have revealed a strong correlation between the prevalence and development of breast cancer and abnormal expression of ceRNAs. [24].

The purpose of the present study was to use *in silico* analysis to find miRNA-associated ceRNAs that may be used as BC biomarkers. The other objective was to find those which also included ceRNAs and T-UCRs. Thus, it will be possible to identify new potential biomarkers supporting the diagnosis and diagnosis of BC. In this study, 40 miRNAs associated with BC (MCF-7 cells), which we determined in our previous study using the miRWalk database, are shown in Table 1. 1009 genes simultaneously targeted by these 40 miRNAs have been identified. Genes with a ComiR score above 0.911 are shown Table 2. [25].

For the matching of breast cancer-associated ceRNA to genes including T-UCR, genes with T-UCR in exon regions were selectively identified according to Bejerano et al. (Table 3) [11]. Using the gene expression profiling database GEPIA, genes with notable expression variations between breast cancer and normal breast tissue were found among breast cancer-associated ceRNAs, including T-UCR. In addition, correlation analysis was performed using the same database [12].

The present findings revealed that the expression of the *NFAT5* and *CLK3* genes in BC was statistically considerably lower than in healthy breast tissue (Figure 2). Others did not exhibit a statistically relevant pattern of differential expression. In addition, Spearman correlation analysis test determined that *NFAT5* and *CLK3* genes were associated with BC (Figure 3). According to the literature review, it was seen that *NFAT5* and *CLK3* genes were not experimentally detected in BC and their relationship with this cancer type was not determined. This study shows that these two genes may be associated with BC. Then, the genes with remarkable expression differences between BC and normal breast tissues were included from MCF7-associated ceRNAs that included. The *NFAT5* and *CLK3* genes were significantly less expressed in BC than in normal breast tissues according to the analysis in this study. On the other hand, other genes did not show any significant differences in expression pattern. According to the findings of the Spearman correlation analysis, *NFAT5* and *CLK3* genes were shown to have remarkable relationship with BC.

The *NFAT* family consists of five transcription factors, and *NFAT5* is an osmotic stress transcription factor [26]. The role of *NFAT5* is to stimulate the synthesis of transmembrane transporters of ions and osmolytes at the gene level. Thus, osmotic stress responses see a coordination function [27]. It has also been reported that *NFAT5* modulates angiogenesis, invasion, glycolysis and osmotic stress, and is responsible for the regulation of many types of cancer [28, 29]. *NFAT5* specifically transcriptionally regulates calcium-binding protein S100A4 and vascular endothelial growth factor C (VEGF-C). Since *NFAT5* regulates many genes transcriptionally, it is stated that *NFAT5* probably has a key role in breast cancer [30, 31]. The signals and metastatic processes that induce *NFAT5* expression in metastatic BC have not been fully determined [32]. These findings imply a causal role for "constitutive activation" or elevated *NFAT5* transcriptional activity in the pathogenesis of BC. For this reason, *in silico* analysis results will contribute to the determination of the function of *NFAT5* in the metastatic process in BC.

*CDC-like kinase 3 (CLK3)* is a nuclear kinase that acts on serine/threonine and tyrosine-containing substrates [33]. *CLK3* modulates RNA splicing by phosphorylating serine/arginine-rich proteins [34]. Although the various tumor activities have not been precisely described, dysregulation of *CLK3* levels has been identified to be a highly penetrating factor in various types of human malignancies [35]. Therefore, the results of the analysis in this study suggest that *CLK3* associated with BC may provide a new therapeutic strategy. In the current investigation, the genes *NFAT5* and *CLK3* were linked to BC, and it was emphasized that these genes may have a role in the development of cancer. According to the analyses in this study, it has been hypothesized that these genes may function as tumor suppressor genes and that their expression is reduced in BC.

## Conclusion

To better understand the molecular pathways behind cancer, many scientists are currently concentrating on ceRNA-based gene regulation. This *in silico* approach will enable the discovery of new undiscovered candidate genes for the pathogenesis of BC. This study confirmed that the *NFAT5* and *CLK3* genes downregulate expression in BC. The *NFAT5* and *CLK3* genes can be used as reliable biomarkers to differentiate between BC patients and healthy people. The assignment of phenotype-specific treatment agents could be aided by the identification of BC and the activation of the *NFAT5* and *CLK3* signaling pathway. According to these *in silico* results, we identified two miRNA-related genes as a novel biomarker in BC that could potentially be developed in clinical trials. Future *in vitro* and *in vivo* investigations may benefit from a novel viewpoint from our preliminary findings. These genes might help us understand the specific mechanisms behind BC. However, further and more comprehensive research on this topic is required.

## Acknowledgement

S.Ö.Y. and S.M. planned, designed and performed the research. S.Ö.Y. and S.M. analyzed the data and wrote the manuscript. All authors contributed to editorial changes in the manuscript. All authors read and approved the final manuscript.

## Conflicts of interest

There are no conflicts of interest in this work.

## References

- [1] Ferlay J., Soerjomataram I., Dikshit R., Eser S., Mathers C., Rebelo M., Parkin D.M., Forman D., Bray F., Cancer incidence and mortality worldwide: Sources, methods and major patterns in GLOBOCAN 2012, *Int. J. Cancer.*, 136 (5) (2015) E359–E386.
- [2] Bray F., Ferlay J., Soerjomataram I., Siegel R.L., Torre L.A., Jemal A., Global cancer statistics 2018:GLOBOCAN estimates of incidence and mortality worldwide for 36 cancers in 185 countries, *CA Cancer J Clin.*,68(6) (2018) 394-424.
- [3] Wang L., Early diagnosis of breast cancer, *Sensors.*, 17(7) (2017) 1-20.
- [4] Loh H. Y., Norman B. P., Lai K. S., Rahman N. M. A. N. A., Alitheen N. B. M., Osman M. A., The regulatory role of microRNAs in breast cancer, *Int. J. Mol. Sci.*, 20(19) (2019) 1-27.
- [5] Szczepanek J., Skorupa M., Tretyn A., MicroRNA as a potential therapeutic molecule in cancer, *Cells*, 11(6) (2022) 1-24.
- [6] Jang J. Y., Kim Y. S., Kang K. N., Kim K. H., Park Y. J., Kim, C. W., Multiple microRNAs as biomarkers for early breast cancer diagnosis, *Mol Clin Oncol.*, 14(2) (2021) 1-9.
- [7] Qi X., Zhang D.H., Wu N., Xiao J.H., Wang X., Ma W., CeRNA in cancer: possible functions and clinical implications, *J Med Genet.*, 52(10) (2015) 710-8.

- [8] Fassan M., Dall'Olmo L., Galasso M., Braconi C., Pizzi M., Realdon S., Volinia S., Valeri N., Gasparini P., Baffa R., Souza R.F., Vicentini C., D'Angelo E., Bornschein J., Nuovo G.J., Zaninotto G., Croce C. M., Rugge M., Transcribed ultraconserved noncoding RNAs (TUCR) are involved in Barrett's esophagus carcinogenesis, *Oncotarget*, 5(16) (2014) 7162-71.
- [9] Dweep H., Gretz N., miRWalk2. 0: a comprehensive atlas of microRNA-target interactions, *Nat Methods*, 12 (8) (2015) 697-697.
- [10] Coronello C., Benos P.V., ComiR: combinatorial microRNA target prediction tool, *Nucleic Acids Res.*, 41(W1) (2013) W159-W164.
- [11] Bejerano G., Pheasant M., Makunin I., Stephen S., Kent W.J., Mattick J.S., Haussler D., Ultraconserved elements in the human genome. *Science*, 304(5675) (2004) 1321-5.
- [12] Tang Z., Li C., Kang B., GEPIA: a web server for cancer and normal gene expression profiling and interactive analyses, *Nucleic Acids Res.*, 45(W1) (2017) W98-W102
- [13] Ghoncheh M., Pournamdar Z., Salehiniya H., Incidence and mortality and epidemiology of breast cancer in the world. *Asian Pac. J. Cancer Prev*, 17(sup3) (2016) 43-46.
- [14] Bettaieb A., Paul C., Plenchette S., Shan J., Chouchane L., Ghiringhelli F., Precision Medicine in Breast Cancer: Reality or Utopia? *J Transl Med*, 15 (1) (2017) 1-13.
- [15] Ahmed K. T., Sun J., Chen W., Martinez I., Cheng S., Zhang W., Zhang W., In silico model for miRNA-mediated regulatory network in cancer. *Brief. Bioinform.*, 22(6), 2021, 1–13.
- [16] Sadeghi M., Cava C., Mousavi P., Sabetian S., Insilico-based identification of survival-associated lncRNAs, mRNAs and, miRNAs in breast cancer, *Research Square*, (2022) 1-21.
- [17] Kartha R.V., Subramanian S., Competing endogenous RNAs (ceRNAs): new entrants to the intricacies of gene regulation, *Front Genet.*, 5 (8) (2014) 1-9.
- [18] Akkaya Z.Y., Dinçer P., The new era in therapeutic approaches: Non-coding RNAs and diseases, *Marmara Medical Journal*, 26 (1) (2013) 5-10.
- [19] Salmena L., Poliseno L., Tay Y., Kats L., Pandolfi P.P., A ceRNA Hypothesis: The Rosetta Stone of a Hidden RNA Language? *Cell*, 146 (3) (2011) 353–358.
- [20] Ebert M.S., Neilson J.R., Sharp P.A., MicroRNA sponges: Competitive inhibitors of small RNAs in mammalian cells, *Nat. Methods*, 4 (9) (2007) 721–726.
- [21] Arvey A., Larsson E., Sander C., Leslie C.S., Marks D.S., Target mRNA abundance dilutes microRNA and siRNA activity. *Mol. Syst. Biol.*, 6 (1) (2010) 1-7.
- [22] Ebert M.S., Sharp P.A., Emerging Roles for Natural MicroRNA Sponges, *Curr. Biol.*, 20 (19) (2010) R858–R861.
- [23] Sen R., Ghosal S., Das S., Balti S., Chakrabarti J., Competing endogenous RNA: the key to posttranscriptional regulation. *Sci. World J.*, 2014 (896206) (2014) 1-7.
- [24] Wu D., Zhu J., Fu Y., Li C., Wu B., lncRNA HOTAIR promotes breast cancer progression through regulating the miR-129-5p/FZD7 axis. *Cancer Biomarkers*, 30(2) (2021) 203–212.
- [25] Misir S., Hepokur C., Aliyazicioglu Y., Enguita F. J., Biomarker potentials of miRNA-associated circRNAs in breast cancer (MCF-7) cells: an in vitro and in silico study, *Mol Biol Rep.*, 48(3) (2021) 2463-2471.
- [26] Brown T.C., Murtha T.D., Rubinstein J.C., Korah R., Carling T., SLC12A7 alters adrenocortical carcinoma cell adhesion properties to promote an aggressive invasive behavior. *Cell Commun Signal.*, 16(1) (2018) 1-13.
- [27] Burg M.B., Ferraris J.D., Dmitrieva N.I., Cellular response to hyperosmotic stresses. *Physiol Rev.*, 87(4) (2007) 1441-1474.
- [28] Chen M., Sastry S.K., O'Connor K.L., Src kinase pathway is involved in NFAT5-mediated S100A4 induction by hyperosmotic stress in colon cancer cells, *Am J Physiol Cell Physiol.*, 300(5) (2011) C1155-C1163.
- [29] Küper C., Beck F.X., Neuhofer W., NFAT5-mediated expression of S100A4 contributes to proliferation and migration of renal carcinoma cells, *Front Physiol.*, 5 (293) (2014) 1-10.
- [30] Mishra S.K., Siddique H.R., Saleem M., S100A4 calcium-binding protein is key player in tumor progression and metastasis: preclinical and clinical evidence, *Cancer Metastasis Rev.*, 31 (2012) 163–172.
- [31] Su J.L., Yen C.J., Chen P.S., Chuang S.E., Hong C.C., Kuo I.H., Chen H.Y., Hung M.C., Kuo M.L., The role of the VEGF-C/VEGFR-3 axis in cancer progression, *Br J Cancer*. 96 (2007) 541–545.
- [32] Remo A., Simeone I., Pancione M., Parcesepe P., Finetti P., Cerulo L., Bensmail H., Birnbaum D., Van Laere S.J., Colantuoni V., Bonetti F., Bertucci F., Manfrin E., Ceccarelli M., Systems biology analysis reveals NFAT5 as a novel biomarker and master regulator of inflammatory breast cancer, *J. Transl. Med.*, 13(1) (2015) 1-13.
- [33] Nayler O., Stamm S., and Ullrich A., Characterization and comparison of four serine- and arginine-rich (SR) protein kinases, *Biochem. J.*, 326 (1997) 693–700.
- [34] Cesana M., Guo M.H., Cacchiarelli D., Wahlster L., Barragan J., Doulatov S., Vo L.T., Salvatori B., Trapnell C., Clement K., Cahan P., Tsanov K. M., Sousa P.M., Tazon-Vega B., Bolondi A., Giorgi F.M., Califano A., Rinn J.L., Meissner A., Hirschhorn J.N., Daley G. Q., A CLK3-HMGA2 alternative splicing axis impacts human hematopoietic stem cell molecular identity throughout development, *Cell Stem Cell.*, 22 (e7) (2018) 575–588.
- [35] Bowler E., Porazinski S., Uzor S., Thibault P., Durand M., Lapointe E., Rouschop K.M.A., Hancock J., Wilson I., and Ladomery M., Hypoxia leads to significant changes in alternative splicing and elevated expression of CLK splice factor kinases in PC3 prostate cancer cells, *BMC Cancer.*, 18 (2018) 1-11.